High-throughput Screening and Identification of Potent Broad-spectrum Inhibitors of Coronaviruses

Liang Shen[1#], Junwei Niu[1#], Chunhua Wang[2], Baoying Huang[1], Wenling Wang[1], Na Zhu[1], Yao Deng[1], Huijuan Wang[1], Fei Ye[1], Shan Cen[3], Wenjie Tan[1]*

[1]NHC Key Laboratory of Biosafety, Ministry of Health, National Institute for Viral Disease Control and Prevention, China CDC, Beijing 102206, China

[2]National Institutes for Food and Drug Control, Beijing 100050, China

[3]Department of Immunology, Institute of Medicinal Biotechnology, Chinese Academy of Medical Sciences, Beijing 100050, China

Running title: Broad-spectrum inhibitors against CoV infection

Word count of abstract: 233

Word count of main text: 4519

#L. Shen and J. Niu contributed equally to this work.

* Correspondence: W. Tan, NHC Key Laboratory of Biosafety, National Institute for Viral Disease Control and Prevention, Chinese Center for Disease Control and Prevention, 155 Changbai road, Changping district, Beijing, CA 102206 (tanwj28@163.com).Phone/Fax:08610-58900878

Disclaimer. The findings and conclusions in this report are those of the authors and do not necessarily represent the official position of the Centers for Disease Control and Prevention (CDC).

ABSTRACT

Coronaviruses (CoVs) act as cross-species viruses and have the potential to spread rapidly into new host species and cause epidemic diseases. Despite the severe public health threat of severe acute respiratory syndrome coronavirus and Middle East respiratory syndrome CoV (MERS-CoV), there are currently no drugs available for their treatment; therefore, broad-spectrum inhibitors of emerging and endemic CoVs are urgently needed. To search for effective inhibitory agents, we performed high-throughput screening (HTS) of a 2,000-compound library of approved drugs and pharmacologically active compounds using the established genetically engineered human CoV OC43 (HCoV-OC43) strain expressing *Renilla* luciferase (rOC43-ns2Del-Rluc) and validated the inhibitors using multiple genetically distinct CoVs *in vitro*. We screened 56 hits from the HTS data and validated 36 compounds *in vitro* using wild-type HCoV-OC43. Furthermore, we identified seven compounds (lycorine, emetine, monensin sodium, mycophenolate mofeti, mycophenolic acid, phenazopyridine, and pyrvinium pamoate) as broad-spectrum inhibitors according to their strong inhibition of replication by four CoVs in vitro at low-micromolar concentrations. Additionally, we found that emetine blocked MERS-CoV entry according to pseudovirus-entry assays, and that lycorine protected BALB/c mice against HCoV-OC43-induced lethality by decreasing viral load in the central nervous system. This represents the first demonstration of *in vivo* real-time bioluminescence imaging to monitor the effect of lycorine on the spread and distribution of HCoV-OC43 in a mouse model. These results offer critical information supporting the development of an effective therapeutic strategy against CoV infection.

52 **IMPORTANCE**

53 Currently, there is no approved therapy to treat coronavirus infection; therefore,
54 broad-spectrum inhibitors of emerging and endemic CoVs are needed. Based on our
55 high-throughput screening assay using a compound library, we identified seven compounds
56 with broad-spectrum efficacy against the replication of four CoVs *in vitro*. Additionally, one
57 compound (lycorine) was found to protect BALB/c mice against HCoV-OC43-induced
58 lethality by decreasing viral load in the central nervous system. This inhibitor might offer
59 promising therapeutic possibilities for combatting novel CoV infections in the future.

60

Introduction

Emerging viruses are difficult to control, because they periodically cycle in and out of humans and livestock; therefore, effective vaccines and antivirals are urgently needed. Coronaviruses (CoVs) represent a group of enveloped, positive-sense, single-stranded viruses with large genomes (27–33 kb) and capable of causing respiratory, enteric, hepatic, and neurological diseases of varying severities in diverse animal species, including humans. All CoVs have a similar genome organization: approximately two-thirds of the 5′-proximal genome contains the ORF1a/b replicase gene, and the remainder encodes the spike, envelope, membrane, and nucleocapsid structural proteins along with several accessory proteins. CoVs belong to the family *Coronaviridae* in the order *Nidovirales* (1) and are divided into four genera: alpha-, beta-, gamma-, and delta-CoVs. Only alpha- and beta-CoVs can infect humans, with four CoVs currently known to be prevalent: human CoV 229E (HCoV-229E), HCoV-OC43, HCoV-HKU1, and HCoV-NL63. Severe acute respiratory syndrome CoV (SARS-CoV) and Middle East respiratory syndrome CoV (MERS-CoV) (2, 3) are considered the most emergent CoVs.

CoV infections are difficult to prevent and cure. Although CoV-replication machinery exhibits substantial proofreading activity, estimates of the nucleotide-mutation rate in CoVs are moderate-to-high relative to other single-stranded RNA viruses. Additionally, the large RNA genome in CoVs allows for extra plasticity in genome modification by recombination (4–6). Moreover, many animal CoVs cause long-term or persistent enzootic infections, which increase the probability of infecting a new host species. SARS-CoV and MERS-CoV are recent examples of newly emergent CoVs that cause severe human diseases (7, 8). Several

drugs, such as ribavirin, lopinavir–ritonavir, interferon, and corticosteroids, have been used to treat patients infected with SARS-CoV or MERS-CoV (9–12). However, contradictory findings on their efficacy and concerns over tolerability and clinical benefit have limited the use of antiviral therapeutics for CoVs. Although substantial effort has focused on identifying antivirals for CoV treatment, no approved therapeutic (drug or biological agent) is currently available for the prophylaxis or treatment of CoV-related disease. Treatments for emerging CoV diseases rely upon supportive care and the judicious use of limited quantities of experimental therapeutics (13). Moreover, the lack of effective drugs, high morbidity and mortality rates caused by the virus, and potential of epidemic spread highlight the need for new broad-spectrum anti-CoV drugs, especially given the likelihood of infection by novel CoVs (13).

Several recent studies highlighted potential broad-spectrum inhibitors against CoVs (13–17). de Wilde et al. (14) identified numerous potent MERS-CoV inhibitors through screening of a United States Food and Drug Administration (FDA)-approved drug library. Interestingly, all of the screened compounds were also capable of inhibiting the replication of SARS-CoV and HCoV-229E. Dyall et al. (15) also screened 27 compounds with activity against both MERS-CoV and SARS-CoV from a 290-compound library; however, the half-maximal effective concentration (EC_{50}) values of most of these drugs were relatively high *in vitro* but were not assessed *in vivo*, making their clinical utility questionable. Müller et al. (16) found that silvestrol was a potent and non-toxic inhibitor of cap-dependent viral mRNA translation in CoV-infected human primary cells, with EC_{50} values of 1.3 nM and 3 nM for MERS-CoV and HCoV-229E, respectively. Notably, Sheahan et al. (17) showed that a

nucleotide prodrug (GS-5734) could inhibit SARS-CoV and MERS-CoV replication in multiple *in vitro* systems at submicromolar half-maximal inhibitory concentration (IC_{50}) values. Furthermore, the prophylactic and early therapeutic administration of GS-5734 significantly reduced the lung viral load and improved clinical signs of disease, as well as respiratory function, in a mouse model of SARS-CoV pathogenesis, further supporting the development of GS-5734 as a broad-spectrum therapeutic to protect against CoVs.

HCoV-OC43, along with SARS-CoV and MERS-CoV, all belong to beta-CoVs and show a high degree of conservation of essential functional domains, especially within 3CLpro, RdRp, and the RNA helicase, which might represent potential targets for broad-spectrum anti-CoV drugs. We recently reported that a genetically engineered CoV strain (HCoV-OC43) expressing *Renilla* luciferase (Rluc; rOC43-ns2Del-Rluc) facilitates high-throughput screening (HTS) for broad-spectrum anti-CoV agents and quantitative analysis of CoV replication (18). In the present study, we performed HTS of a 2,000-compound library containing FDA-approved drugs and pharmacologically active compounds and assessed broad-spectrum anti-CoV activity *in vitro* and *in vivo* in an experimental infection mouse model. This comprehensive screening and assessment provided new candidate inhibitors to effectively treat infections by existing CoVs, as well as those by emergent strains in the future.

Results

HTS of anti-HCoV-OC43 compounds. Optimal screening conditions were established using the rOC43-ns2Del-Rluc reporter virus to infect BHK-21 cells in 96-well plates [multiplicity of infection (MOI) = 0.01; 10,000 cells/well]. Under this condition, the coefficient of

127 variation and Z factor were 2.9% and 0.86, respectively, demonstrating that the assay was
128 robust and suitable for HTS.

129 A schematic of the HTS strategy is depicted in Figure 1A. In the primary screening from
130 the 2,000-compound library under a concentration of 10 μM, 56 hits were found to
131 significantly inhibit rOC43-ns2Del-Rluc replication (Figure 1B; red and yellow squares),
132 with ≥70% reduced Rluc activity and ≤80% cytotoxicity, including 12 FDA-approved drugs.
133 To obtain more potent inhibitors and exclude the possibility that the observed antiviral
134 activity was specific to rOC43-ns2Del-Rluc, we confirmed the antiviral activity of the 56 hits
135 against HCoV-OC43-WT by quantitative reverse transcription (qRT)-PCR under a lower
136 concentration (5 μM), which confirmed the antiviral activity of 36 compounds (Figure 1B;
137 yellow squares).

138

139 **Identification of broad-spectrum anti-CoV inhibitors *in vitro*.** Because only alpha- and
140 beta-CoVs infect humans, we focused on three other CoVs [MERS-CoV (beta-CoV), mouse
141 hepatitis virus (MHV)-A59 (beta-CoV), and HCoV-NL63 (alpha-CoV)] to assess the
142 broad-spectrum antiviral activity of the 36 compounds using eight-point dose-response
143 confirmation (15). We identified 17 compounds that inhibited the replication of HCoV-NL63
144 (EC_{50} < 5 μM), which is an alpha-CoV that usually causes the common cold, whereas 13 and
145 12 compounds inhibited MERS-CoV and MHV-A59 replication (EC_{50} < 5 μM), respectively
146 (Table 1). Moreover, we newly identified nine compounds **(**phenazopyridine, lycorine,
147 pyrvinium pamoate, monensin sodium, cetylpyridinium chloride, oligomycin, loperamide,
148 harmine, and conessine) as exhibiting antiviral activity against severe CoV (MERS-CoV)

(Table 1). Interestingly, the following seven compounds inhibited the replication of all CoVs with EC_{50} < 5 μM: lycorine, emetine, phenazopyridine, mycophenolic acid, mycophenolate mofetil, pyrvinium pamoate, and monensin sodium (Table 1; bold).

These seven broad-spectrum inhibitors suppressed the replication of all CoVs in a dose-dependent manner and with low EC_{50} values (Figure 2). Lycorine, an active alkaloid from the common folk medicine *Lycoris radiata* (*Amaryllidaceae*) has been investigated for its multifunctional biological effects, including anticancer, antimalarial, antiviral, antibacterial, and anti-inflammatory activities (19-23). Lycorine showed potent anti-CoV activity, with EC_{50} values ranging from 0.15 μM to 1.63 μM. Moreover, the selective index (SI) of lycorine for HCoV-OC43 was calculated at 29.13, indicating its potent anti-HCoV-OC43 activity (Figure 2A). Emetine is an active principal of ipecac and inhibits the replication of both DNA and RNA viruses. Additionally, emetine displayed potent anti-CoV activity and the strongest anti-MERS-CoV activity among the top seven inhibitors, with an EC_{50} value of 0.34 μM and SI of 9.06 (Figure 2B). Mycophenolic acid (an immunosuppressant) exerted a significant inhibitory effect on HCoV-OC43 replication, with an EC_{50} of 1.95 μM, and showed stronger anti-HCoV-NL63 activity than the others (EC_{50} = 0.18 μM and SI = 19.11) (Figure 2E). Mycophenolate mofetil, a derivative of mycophenolic acid, showed a similar antiviral effect on the four CoVs as that from mycophenolic acid, suggesting that the two drugs might harbor similar core structures and antiviral mechanisms (Figure 2C and E). Moreover, phenazopyridine, a widely used urinary analgesic, also displayed strong broad-spectrum anti-CoV activity for the first time, especially against MHV-A59 (EC_{50} = 0.77 μM and SI > 25.97) (Figure 2D). Pyrvinium pamoate is an

171 FDA-approved anthelminthic drug and a potent inhibitor of WNT signaling, suggested to
172 occur through direct activation of protein kinase CK1α (24). Pyrvinium pamoate inhibited the
173 replication of all CoVs and displayed low toxicity [50% cytotoxic concentration (CC_{50}) >19
174 μM] (Figure 2F). Finally, monensin sodium, previously shown to inhibit the formation of
175 gamma-CoV infectious bronchitis virus (IBV), inhibited all CoVs at low EC_{50} values and
176 displayed low toxicity (Figure 2G). Although the specific antiviral mechanisms of these
177 seven inhibitors against CoVs are unknown, they showed potential as new antivirals for the
178 treatment of infections caused by a range of CoVs.
179
180 **Validation of anti-CoV activity.** We verified the antiviral activity of the seven inhibitors
181 against HCoV-OC43 by indirect immunofluorescence assay (IFA) and western blot. As
182 shown in Figure 3A, all seven inhibitors significantly suppressed HCoV-OC43 replication as
183 compared with the control [dimethyl sulfoxide (DMSO)] and with a >90% inhibitory effect
184 for most compounds, except for monensin sodium. Additionally, we observed inhibitory
185 activity when the cells were treated with the inhibitors after viral infection, resulting in
186 significantly reduced levels of HCoV-OC43 nucleocapsid protein (Figure 3B). Although the
187 inhibitory effect of mycophenolic acid differed according to IFA and western blot results, the
188 seven inhibitors clearly suppressed HCoV-OC43 replication.
189
190 **Emetine inhibited MERS-CoV entry.** Viral entry is an essential step of the viral life cycle
191 and is thus an attractive target for therapy. Inhibition of this step can block viral propagation
192 at an early stage of infection, thereby minimizing the chance for the virus to evolve and

193 acquire drug resistance. Therefore, we tested the effect of the seven screened inhibitors on
194 CoV entry using a pseudotype virus with a human immunodeficiency virus (HIV)-1
195 backbone but expressing the spike protein of MERS-CoV in order to generate dose-response
196 curves. Measurement of the inhibition percentage showed that only emetine was an entry
197 inhibitor that blocked MERS-CoV-S-mediated infection, with luciferase activity reduced
198 50-fold as compared with the control and an EC_{50} value of 0.16 μM (Figure 4).
199
200 **Antiviral activity of lycorine against lethal HCoV-OC43 infection *in vivo*.** HCoV-OC43
201 infects neurons and causes encephalitis in mice, with this model previously used for anti-CoV
202 drug evaluation (25). Moreover, this model was convenient based on the lack of need for
203 three biological facilities as opposed to experiments involving SARS-CoV or MERS-CoV.
204 Therefore, we used this model to evaluate the in vivo antiviral activity of the seven inhibitors.
205 Intracerebral or intranasal inoculation of HCoV-OC43 results in acute-onset severe
206 neurological illness and causes death, with high levels of viral replication in the brain [titer >
207 10^6 50% tissue culture infective dose ($TCID_{50}$)/mL] at 3 to 5 days after infection (26–29).
208 Briefly, female BALB/c mice (12-days old) were inoculated via the intranasal route with 100
209 $TCID_{50}$ of HCoV-OC43-WT and treated with the seven inhibitors for 14 days, and their
210 survival was monitored for up to 20 days. The inhibitor doses and regimens were selected
211 based on acute-toxicity assessments. Emetine was used at 5 mg/kg, and chloroquine was used
212 as the positive control, which showed antiviral activity at 30 mg/kg. All mice in the
213 phosphate-buffered saline (PBS)/DMSO-treated group died within 6 days after
214 HCoV-OC43-WT challenge (Figure 5A). By contrast, 83.3% of mice in the lycorine-treated

group were still alive at 20-days post-inoculation ($p < 0.001$), similar to the survival rate of the chloroquine-treated group (Figure 5A). Additionally, viral loads in the brain and spinal cord were under the limit of detection in the lycorine-treated group (Figure 5B), and immunohistochemistry (IHC) of mouse-brain coronal sections showed that HCoV-OC43 nucleocapsid protein was present only in the PBS/DMSO-treated group but not in the lycorine-treated group (Figure 5C).

Lycorine blocked the spread of rOC43-ns2Del-Rluc in the mouse brain. To more closely monitor the effect of lycorine on the spread and replication of HCoV-OC43 in the mouse central nervous system in real-time, we used bioluminescence imaging (BLI) based on its important advantages of intrinsically low background signal combined with very high sensitivity for monitoring light emission *in vivo*. As expected, PBS/DMSO-treated mice showed gradually increasing signal intensity post-inoculation, whereas no signal was detected in the brains of lycorine-treated mice (Figure 6A). These observations were confirmed by the ~2×10^5-fold higher Rluc activity in the PBS/DMSO-treated mice than in the lycorine-treated mice. Therefore, lycorine showed promise as an anti-CoV agent (Figure 6B).

Discussion

The SARS epidemic in 2003 and the ongoing MERS-CoV outbreak highlight the inadequacy of available treatments for life-threatening zoonotic CoV infections in humans. Indeed, no specific antiviral agent or vaccine is currently available for human or zoonotic CoV infections, despite the extensive research efforts triggered by the SARS outbreak (30–32). Several FDA-approved drugs (ritonavir, lopinavir, nelfinavir, mycophenolic acid, and ribavirin)

237 inhibit the entry and/or replication of MERS-CoV, SARS-CoV, or other human CoVs in
238 multiple cell lines; however, their antiviral efficacy *in vivo* remains unknown (16, 32–37). To
239 date, few small molecules have demonstrated anti-CoV activity in animal models of CoV
240 infection (17, 38-39), and most of the available anti-CoV drugs that target structural proteins
241 might not be effective against other CoVs. For example, the human monoclonal antibodies
242 and antiviral peptides that block virus–host cell binding typically have a limited breadth of
243 protection due to the antigenic diversity in the CoV spike glycoprotein (40, 41). It is worth
244 mentioning that combining antiviral peptides with interferon-β (40) or combination therapy
245 with different humanized or human monoclonal antibodies targeting non-cross-resistant
246 epitopes (42) can enhance antiviral therapeutic effects. There are also several reports of the
247 enhanced therapeutic effects of combinations of other antiviral agents for the treatment of
248 MERS-CoV. These results indicated that combined use of different antiviral agents might be
249 synergistic in their treatment of CoV infection.

250 Here, we identified seven potent broad-spectrum anti-CoV agents, among which
251 lycorine was confirmed as showing strong anti-CoV activity *in vivo*. Our results suggested
252 that FDA-approved drugs can be used for the prophylaxis of severe or lethal CoV infections,
253 thereby greatly facilitating the rapid and rational development of anti-CoV agents with
254 desirable pharmacokinetic and biodistribution properties.

255 The criteria for the inhibition rate associated with the signals in the antiviral HTS
256 screening assay ranged from ~30% to ~90% according to different references, with more
257 primary hits but fewer efficacy hits screened when the inhibition rate was set to the lower
258 threshold. In our experiment, we focused on screening hits with higher potency; therefore, so

established the inhibition threshold at 70%. Furthermore, we identified several effective hits with a high degree of cytotoxicity under 10 μM in our primary screening, which was why the cytotoxicity value was set to 80%. Finally, we identified 36 compounds exhibiting anti-HCoV-OC43 activity from a library of compounds, two of which (chloroquine and loperamide) were previously reported as exhibiting broad-spectrum anti-CoV activity. Nine compounds (phenazopyridine, lycorine, pyrvinium pamoate, monensin sodium, cetylpyridinium chloride, oligomycin, loperamide, harmine, and conessine) have not previously been demonstrated as exhibiting antiviral activity against MERS-CoV, thereby offering new therapeutic possibilities for this severe CoV. Furthermore, seven compounds (lycorine, emetine, monensin sodium, mycophenolate mofetil, mycophenolic acid, phenazopyridine, and pyrvinium pamoate) showed inhibitory activity against multiple genetically distinct CoVs *in vitro* at low-micromolar concentrations (EC_{50} values ranging from 0.12 to 3.81 μM). Among these, lycorine is an alkaloid isolated from *Amaryllidaceae* plants and reportedly exhibits anticancer, antiplasmodial, antitrypanosomal, anti-inflammatory, analgesic, and emetic activities (43-45). Lycorine inhibits the replication of poliomyelitis virus, herpes simplex virus (type I), Bunyamwera virus, West Nile virus, dengue virus, and SARS-CoV *in vitro*, although the mechanism remains to be elucidated (46–49). Liu et al. (50) demonstrated the ability of lycorine to reduce the mortality of human enterovirus 71-infected mice by inhibiting viral replication. Furthermore, Guo et al. (51) evaluated a total of 32 lycorine derivatives, demonstrating that 1-acetyllycorine suppressed enterovirus 71 and hepatitis C virus replication in various cells. Moreover, drug-resistance analysis revealed that 1-acetyllycorine targeted a phenylalanine (F76) in the viral proteases.

281 Lycorine also exhibits strong activities against influenza A virus H5H1 *in vitro* and delays the
282 export of nucleoprotein from the nucleus to the cytoplasm during replication (52). However,
283 the potential mechanism of lycorine against CoVs requires further exploration, and its
284 potential selection for drug-resistant strains must be assessed. We found no reports
285 concerning whether its use in combination enhances the antiviral efficacy of lycorine.
286 Additionally, Emetine is a drug mainly used as both an anti-protozoal and an emetic (53),
287 with a number of groups recently reporting new antiviral roles for emetine. Emetine is
288 reportedly a potent inhibitor that suppresses the replication of several RNA viruses (dengue
289 virus and HIV) without generating drug-resistant variant viruses (54–56). We noted that
290 emetine inhibits human cytomegalovirus (HCMV) replication by disrupting the
291 HCMV-induced interaction between p53 and the E3-ubiquitin ligase MDM2 (57). Moreover,
292 a recent study revealed emetine as an inhibitory modulator of rabies-virus axonal transport
293 via a mechanism independent of protein-synthesis inhibition (58). Furthermore, Yang et al.
294 (59) demonstrated the emetine inhibits Zika virus (ZIKV) replication via inhibition of ZIKV
295 NS5 polymerase activity and disruption of lysosomal function. In the present study, our
296 preliminary result indicated that emetine inhibited MERS-CoV entry. Interestingly, the
297 immunosuppressant mycophenolic acid and its derivative mycophenolate mofetil, which
298 suppress MERS-CoV replication (33), also inhibited HCoV-OC43 replication (EC_{50} = 1.95
299 and 1.58 μM, respectively). However, a previous study showed that MERS-CoV-infected
300 common marmosets treated with mycophenolate mofetil had more severe forms of disease
301 and higher lung viral loads than those of untreated animals, and renal-transplant recipients on
302 maintenance mycophenolate mofetil therapy reportedly developed severe or fatal MERS (60).

303 Therefore, these two inhibitors are unlikely to be useful against CoV infections. Monensin
304 sodium, which affects IBV and MHV-A59 assembly (61, 62), was also identified as an
305 inhibitor of other CoVs (MERS-CoV, HCoV-OC43, and HCov-NL63) in this study.

306 Lycorine showed strong antiviral activity against multiple genetically distinct CoVs *in*
307 *vitro* and protected mice against lethal HCoV-OC43 infection *in vivo*. To our knowledge, this
308 is the first report of the use of BLI to evaluate the effects of antiviral agents on CoV
309 replication and dissemination *in vivo* without the need for sacrificing animals to quantify viral
310 titers and establish the complete pattern of virus dissemination in the central nervous system.
311 However, most of the data and conclusions concerning the antiviral effects of the inhibitors
312 were derived only from one cell line and should be tested in different CoV-replication cell
313 lines in order to exclude the influence of host-cell factors, especially for MERS-CoV, for
314 which there are a larger number of susceptible cell lines (e.g., Huh 7 or Calu3/2B4 cells).
315 Therefore, further *in vitro* and *in viv*o studies are warranted to determine the potential
316 antiviral mechanisms associated with the seven compounds, as well as their clinical efficacy.
317 Additionally, the efficacy of lycorine–interferon combinations should be explored in animal
318 models.

319 Following SARS and MERS, future emerging CoVs will likely pose a threat to public
320 health. Therefore, identification of broad-spectrum inhibitors of SARS-CoV, MERS-CoV, and
321 future emerging CoVs is a research priority. From this perspective, the potent broad-spectrum
322 inhibitors (lycorine and emetine) identified in this study might be effective against CoV
323 infections either as single agents or in combination.

324

325 **Materials and Methods**

326 **Cell lines, viruses, compounds, and antibodies.** BHK-21, Vero-E6, LLC-MK2, DBT,
327 293FT, DPP4-expressing Huh7.5 cells, and 17Cl-1 cells were cultured in Dulbecco's
328 modified Eagle's medium (DMEM; Gibco, Thermo Fisher Scientific, Waltham, MA, USA)
329 supplemented with 10% fetal bovine serum (FBS; Gibco) and incubated at 37°C in an
330 atmosphere containing 5% CO_2.

331 HCoV-OC43 (GenBank accession number: AY391777.1) expressing the Rluc gene
332 (rOC43-ns2Del-Rluc) and derived from an infectious cDNA clone (17) was used for HTS in
333 HBK-21 cells. HCoV-NL63 strain Amsterdam I was used to infect monolayers of LLC-MK2
334 cells at an MOI of 0.01. The MERS-CoV strain EMC was used to infect monolayers of
335 Vero-E6 cells at an MOI of 0.01. The MHV strain A59 was propagated in 17Cl-1 cells, and a
336 plaque assay was performed in monolayers of DBT cells infected with MHV at an MOI of
337 0.01.

338 A 2,000-compound library containing FDA-approved drugs and pharmacologically
339 active compounds was purchased from MicroSource Discovery Systems, Inc. (Gaylordsville,
340 CT, USA) (Table S1).

341 The anti-HCoV-OC43 nucleocapsid protein mouse monoclonal antibody was made
342 in-house. Anti-β-actin (13E5) rabbit monoclonal antibody was obtained from Cell Signaling
343 Technology (Danvers, MA, USA). Infrared IRDye 800CW-labeled goat anti-mouse IgG and
344 680RD-labeled goat anti-rabbit IgG were purchased from LI-COR Biosciences (Lincoln, NE,
345 USA).

346

Viral load assays. MHV titers were quantified by a plaque assay, as described previously (63). Viral genomic RNA from HCoV-OC43, HCoV-NL63, and MERS-CoV was extracted from 50 µL of cell-culture supernatants using a QIAamp viral RNA mini kit (Qiagen, Valencia, CA, USA) and quantified by real-time RT-PCR, as described previously (64, 65). The primer and probe sequences were as follows: q-OC43-F, 5′-GCT CAG GAA GGT CTG CTC C-3′; q-OC43-R, 5′- TCC TGC ACT AGA GGC TCT GC-3′; q-OC43-probe, 5′-FAM-TTC CAG ATC TAC TTC GCG CAC ATC C-TAMRA-3′; q-NL63-F, 5′- AGG ACC TTA AAT TCA GAC AAC GTT CT-3′; q-NL63-R, 5′- GAT TAC GTT TGC GAT TAC CAA GAC T-3′; q-NL63-probe, 5′-FAM-TAA CAG TTT TAG CAC CTT CCT TAG CAA CCC AAA CA-TAMRA-3′; q-MERS-F, 5′- GGC ACT GAG GAC CCA CGT T-3′, q-MERS-R, 5′-TTG CGA CAT ACC CAT AAA AGC A-3′; and q-MERS-probe, 5′-FAM-CCC CAA ATT GCT GAG CTT GCT CCT ACA-TAMRA-3′.

Primary screening assay and secondary confirmation assay. HCoV-OC43 can replicate efficiently in BHK-21 cells, with this cell line commonly used for virus isolation or antiviral-screening assays. Therefore, the primary screening assay was conducted using 10 µM of each compound in BHK-21 cells. We observed no difference in the average Rluc signal between mock controls (only reporter virus added) and DMSO controls. The average control (mock or DMSO control) signal was ~6.3×10^6 luciferase light units, and that for the background (only BHK-21 cells) was ~25 luciferase light units.

Briefly, ~4,000 BHK-21 cells were seeded on 96-well plates in DMEM supplemented with 10% FBS. After overnight incubation in a 5% CO_2 atmosphere at 37°C, each well

369 contained ~10,000 cells. The medium was then replaced with 94 µL DMEM supplemented
370 with 3% FBS, and 1 µL of each compound (diluted in DMSO) was added to the plates at a
371 final concentration of 10 µM (one compound per well) in triplicate. An equal volume of
372 DMSO alone was added to the DMSO control wells (Figure 1A). After incubation for 60 min,
373 5 µL of diluted viral suspension was added to each well (MOI = 0.01) for a final total
374 screening volume of 100 µL/well. The plates were incubated at 37°C for 72 h, and luciferase
375 activity was determined using the Renilla-Glo luciferase assay system (Promega, Madison,
376 WI, USA) according to manufacturer instructions. Antiviral activity was calculated as follows:
377 inhibition of Rluc activity (%) = 100% − [relative luminescence units of compound-treated
378 cells / relative luminescence units of DMSO-treated control cells]. Cytotoxicity was
379 calculated as inhibition of BHK-21 proliferation (%) = 100% − [cell viability of
380 compound-treated cells / cell viability of DMSO-treated control cells]. The EC_{50} value and
381 the compound-specific toxicity (CC_{50}) were calculated with GraphPad Prism 5 software
382 (GraphPad, Inc., La Jolla, CA, USA) using the nonlinear regression model. The Z factor, an
383 assessment of the quality of screening assays, was determined, and compounds were
384 considered effective if they reduced Rluc activity by ≥ 70% and cytotoxicity by ≤ 80%.
385 A confirmation assay was performed using HCoV-OC43-WT treated with the
386 compounds at two concentrations (10 and 5 µM), and viral RNA load was determined by
387 qRT-PCR. To screen hits with higher potency and narrow the screening scope, a compound
388 was considered effective only if the EC_{50} value was <5 µM.
389
390 **Western blot.** BHK-21 cells were lysed by incubation in 0.5% NP-40 buffer for 30 min at

391 4°C. Lysates were separated by sodium dodecyl sulfate polyacrylamide gel electrophoresis
392 and transferred to nitrocellulose membranes, which were blocked with 5% skim milk in PBS
393 for 1 h and incubated with the primary antibody overnight at 4°C. After washing with PBS
394 plus Tween-20 buffer, the membranes were incubated for 1 h with the appropriate secondary
395 antibody and scanned using the Odyssey Infrared imaging System (LI-COR Biosciences).
396
397 **Indirect IFA. BHK-21 cells in 96-well plates were infected with HCoV-OC43-WT (MOI =**
398 **0.01) in the presence of 10 μM of the indicated inhibitors, with chloroquine and DMSO**
399 **used as the positive and negative controls, respectively. At 72-h post-infection, cells were**
400 **fixed in 4% formaldehyde, permeabilized in 0.5% Triton X-100, blocked in 5% bovine**
401 **serum albumin in PBS, and then probed with primary antibodies (anti-HCoV-OC43**
402 **nucleocapsid protein) for 1 h at room temperature. The cells were washed three times with**
403 **PBS and then incubated with fluorescein isothiocyanate-labeled goat anti-mouse IgG**
404 **(Sigma-Aldrich, St. Louis, MO, USA) at a dilution of 1:100 for 1 h. The cells were then**
405 **washed and stained with 4,6-diamidino-2-phenylindole (DAPI; Invitrogen, Carlsbad, CA,**
406 **USA) to detect nuclei. Fluorescence images were obtained and analyzed using a**
407 **fluorescence microscope (TE2000U; Nikon, Melville, NY, USA) with a video**
408 **documentation system.**
409
410 **Cell-viability assay.** Cell viability was assessed by a methyl-thiazolyl-tetrazolium (MTT)
411 assay. After 72 h, MTT was added to a final concentration of 0.5 mg/mL, and cells were
412 incubated for 3 h in a humidified 5% CO_2 incubator at 37°C. The plates were then

centrifuged (500*g*, 10 min), and the supernatant was removed from each well by aspiration with a micropipette. Subsequently, 100 µL of DMSO was added per well, and the plates were gently shaken. The absorbance at 580 nm was detected using a Microelisa Auto Reader MR580 spectrometer (Dynatech Laboratories, Inc., Charlottesville, VA, USA).

MERS-CoV-entry inhibition assay. The inhibitory activity of the selected inhibitors on CoV entry was determined using pseudoviruses, as described previously (41). Briefly, 293FT cells were co-transfected with the plasmids PNL4-3.luc.RE- and pVRC-MERS-S, and the culture supernatant containing sufficient pseudotyped MERS-CoV was collected at 72-h post-transfection. Upon reaching a density of 5,000 cells/well in a 96-well plate, dipeptidyl peptidase 4 (DPP4)-expressing Huh7.5 cells were infected with 200 $TCID_{50}$ of the pseudovirus MERS-CoV in the presence of each inhibitor at different concentrations. The culture medium was renewed with fresh medium containing 2% FBS, and luciferase activity was determined after an additional 48 h of incubation using a Promega GloMax 96 plate luminometer (Promega).

Mice and infection. Twelve-day-old female BALB/c mice were inoculated via the intranasal route with 100 $TCID_{50}$ HCoV-OC43-WT or rOC43-ns2Del-Rluc. After 2 h, the mice were treated with the test compounds in 1× DMSO and PBS buffer. The animals were intraperitoneally injected daily with 10 µL of the compounds (emetine was used at 5 mg/kg, chloroquine was used at 30 mg/kg, and other inhibitors were used at 15 mg/kg), and survival was monitored for 20-days post-inoculation. All procedures involving animals were

435 performed in compliance with the Guide for the Care and Use of Laboratory Animals of the
436 People's Republic of China. The study protocol was approved by the Committee on the
437 Ethics of Animal Experiments of the Chinese Center for Disease Control and Prevention.
438
439 **BLI.** BALB/c mice were infected with rOC43-ns2Del-Rluc and treated with lycorine or
440 DMSO/PBS, followed by immediate anesthetization with 2% isoflurane and intraperitoneal
441 administration of ViviRen In Vivo Renilla Luciferase Substrate (20 μg/g; Promega) at 2-, 3-,
442 and 4-days post-inoculation. The mice were positioned in a specially designed box and placed
443 onto the stage inside the light-tight camera box. Mice were imaged within 5-min
444 post-injection of the substrate, and photon flux was quantitated using Living Image software
445 (PerkinElmer, Waltham, MA, USA).
446
447 **IHC.** Mouse brains were removed at 3-days post-infection and fixed in formalin, and the
448 tissues were processed for IHC, as described previously (66).
449
450 **Statistical analysis**. Differences between groups were examined for statistical significance
451 using Student's *t* test. A $p < 0.05$ was considered statistically significant.
452
453 **Acknowledgments**
454 We thank Dr. Talbot PJ (INRS-Institute Armand-Frappier, Université du Québec, Laval,
455 Québec, Canada) for providing the infectious clone of HCoV-OC43 (WT), Dr. Bart L.
456 Haagmans and Dr. Ron A.M. Fouchier (Erasmus MC, Rotterdam, the Netherlands) for

457 providing MERS-CoV (isolate hCoV-EMC/2012), Dr. Lia van der Hoek (Center for Infection
458 and Immunity Amsterdam, Academic Medical Center, University of Amsterdam, the
459 Netherlands) for providing HCoV-NL63 strain Amsterdam I, and Dr. Hongyu Deng (CAS
460 Key Laboratory of Infection and Immunity, Institute of Biophysics, Chinese Academy of
461 Sciences) for providing MHV strain A59. This work was supported by the National Key
462 Research and Development Program of China (2016YFD0500300 to W.T.,
463 2016YFC1200901to B.H.), and the Megaproject for Infectious Disease Research of China
464 (2016ZX10004001-003 to W.T.). The funders had no role in the study design, data collection
465 and analysis, decision to publish, or preparation of the manuscript.
466

467 **Conflict of interest**

468 All authors have submitted the ICMJE Form for Disclosure of Potential Conflicts of Interest.
469 Conflicts that the editors consider relevant to the content of the manuscript have been
470 disclosed.

471

472 **Author contributions**

473 LS and WT designed the study and wrote the first draft of the manuscript. LS, JN, CW, BH,
474 WW, NZ, YD, HW, and FY conducted the experiments. LS conducted the statistical analysis.
475 LS, SC, and WT performed data interpretation. BH and WT supervised the project.

476 **References**

477 1. Saberi A, Gulyaeva AA, Brubacher JL, Newmark PA, Gorbalenya AE. 2018. A planarian
478 nidovirus expands the limits of RNA genome size. PLoS Pathog. 14(11):e1007314.

479 2. Woo PC, Lau SK, Huang Y, Yuen KY. 2009. Coronavirus diversity, phylogeny and
480 interspecies jumping. Exp Biol Med 234:1117–27.

481 3. Zaki AM, van Boheemen S, Bestebroer TM, Osterhaus AD, Fouchier RA. 2012.
482 Isolation of a novel coronavirus from a man with pneumonia in Saudi Arabia. N Engl J
483 Med 367:1814–20.

484 4. Eckerle LD, Becker MM, Halpin RA, Li K, Venter E, Lu X, Scherbakova S, Graham
485 RL, Baric RS, Stockwell TB, Spiro DJ, Denison MR. 2010. Infidelity of SARS-CoV
486 Nsp14-exonuclease mutant virus replication is revealed by complete genome sequencing.
487 PLoS Pathog 6:e1000896.

488 5. Pyrc K, Dijkman R, Deng L, Jebbink MF, Ross HA, Berkhout B, van der Hoek L. 2006.
489 Mosaic structure of human coronavirus NL63, one thousand years of evolution. J Mol
490 Biol. 364:964-73.

491 6. Su S, Wong G, Shi W, Liu J, Lai ACK, Zhou J, Liu W, Bi Y, Gao GF. 2016.
492 Epidemiology, Genetic Recombination, and Pathogenesis of Coronaviruses. Trends
493 Microbiol. 24:490-502.

494 7. de Wit E, van Doremalen N, Falzarano D, Munster VJ. 2016. SARS and MERS: Recent
495 insights into emerging coronaviruses. Nat Rev Microbiol 14:523–34.

496 8. Müller MA, Meyer B, Corman VM, Al-Masri M, Turkestani A, Ritz D, Sieberg A,
497 Aldabbagh S, Bosch BJ, Lattwein E, Alhakeem RF, Assiri AM, Albarrak AM,

Al-Shangiti AM, Al-Tawfiq JA, Wikramaratna P, Alrabeeah AA, Drosten C, Memish ZA. 2015. Presence of Middle East respiratory syndrome coronavirus antibodies in Saudi Arabia: A nationwide, cross-sectional, serological study. Lancet Infect Dis 15:559–64.

9. Loutfy MR, Blatt LM, Siminovitch KA, Ward S, Wolff B, Lho H, Pham DH, Deif H, LaMere EA, Chang M, Kain KC, Farcas GA, Ferguson P, Latchford M, Levy G, Dennis JW, Lai EK, Fish EN. 2003. Interferon alfacon-1 plus corticosteroids in severe acute respiratory syndrome: a preliminary study. JAMA 290:3222–8.
10. Lee N, Hui D, Wu A, Chan P, Cameron P, Joynt GM, Ahuja A, Yung MY, Leung CB, To KF, Lui SF, Szeto CC, Chung S, Sung JJ. 2003. A major outbreak of severe acute respiratory syndrome in Hong Kong. N Engl J Med 348:1986–94.
11. Shalhoub S, Farahat F, Al-Jiffri A, Simhairi R, Shamma O, Siddiqi N, Siddiqi N, Mushtaq A. 2015. IFN-α2a or IFN-β1a in combination with ribavirin to treat Middle East respiratory syndrome coronavirus pneumonia: a retrospective study. J Antimicrob Chemother 70:2129–32.
12. Booth CM, Matukas LM, Tomlinson GA, Rachlis AR, Rose DB, Dwosh HA, Walmsley SL, Mazzulli T, Avendano M, Derkach P, Ephtimios IE, Kitai I, Mederski BD, Shadowitz SB, Gold WL, Hawryluck LA, Rea E, Chenkin JS, Cescon DW, Poutanen SM, Detsky AS. 2003. Clinical features and short-term outcomes of 144 patients with SARS in the greater Toronto area. JAMA 289:2801–9.
13. Zumla A, Chan JF, Azhar EI, Hui DS, Yuen KY. 2016. Coronaviruses—Drug discovery and therapeutic options. Nat Rev Drug Discov 15:327–47.
14. de Wilde AH, Jochmans D, Posthuma CC. 2014. Screening of an FDA-approved

compound library identifies four small-molecule inhibitors of Middle East respiratory syndrome coronavirus replication in cell culture. Antimicrob Agents Chemother 58:4875–84.

15. Dyall J, Coleman CM, Hart BJ, Venkataraman T, Holbrook MR, Kindrachuk J, Johnson RF, Olinger GG Jr, Jahrling PB, Laidlaw M, Johansen LM, Lear-Rooney CM, Glass PJ6, Hensley LE, Frieman MB. 2014. Repurposing of clinically developed drugs for treatment of Middle East respiratory syndrome coronavirus infection. Antimicrob Agents Chemother 58:4885-93.
16. Müller C, Schulte FW, Lange-Grünweller K, Obermann W, Madhugiri R, Pleschka S, Ziebuhr J, Hartmann RK, Grünweller A. 2018. Broad-spectrum antiviral activity of the eIF4A inhibitor silvestrol against corona- and picornaviruses. Antiviral Res. 150:123-129.
17. Sheahan TP, Sims AC, Graham RL, Menachery VD, Gralinski LE, Case JB, Leist SR, Pyrc K, Feng JY, Trantcheva I, Bannister R, Park Y, Babusis D, Clarke MO, Mackman RL, Spahn JE, Palmiotti CA, Siegel D, Ray AS, Cihlar T, Jordan R, Denison MR, Baric RS. 2017. Broad-spectrum antiviral GS-5734 inhibits both epidemic and zoonotic coronaviruses. Sci Transl Med 9:pii: eaal3653.
18. Shen L, Yang Y, Ye F, Liu G, Desforges M, Talbot PJ, Tan W. 2016. Safe and Sensitive Antiviral Screening Platform Based on Recombinant Human Coronavirus OC43 Expressing the Luciferase Reporter Gene. Antimicrob Agents Chemother 60:5492-503.
19. Evidente A, Cicala MR, Giudicianni I, Randazzo G, Riccio R. 1983. 1H and 13C NMR analysis of lycorine and α-dihydrolycorine. Phytochemistry 22:581-4.

20. Liu R, Cao Z, Tu J, Pan Y, Shang B, Zhang G, Bao M, Zhang S, Yang P, Zhou Q. 2012. Lycorine hydrochloride inhibits metastatic melanoma cell-dominant vasculogenic mimicry. Pigment cell & melanoma research 25:630-8.
21. Cho N, Du Y, Valenciano AL, Fernández-Murga ML, Goetz M, Clement J, Cassera MB, Kingston DGI. 2018. Antiplasmodial alkaloids from bulbs of Amaryllis belladonna Steud. Bioorg Med Chem Lett 28:40-2.
22. Bendaif H, Melhaoui A, Ramdani M, Elmsellem H, Douez C, El Ouadi Y. 2018. Antibacterial activity and virtual screening by molecular docking of lycorine from Pancratium foetidum Pom (Moroccan endemic Amaryllidaceae). Microb Pathog 115:138-45.
23. Chen S, Fang XQ, Zhang JF, Ma Y, Tang XZ, Zhou ZJ, Wang JY, Qin A, Fan SW. 2016 Lycorine protects cartilage through suppressing the expression of matrix metalloprotenases in rat chondrocytes and in a mouse osteoarthritis model. Mol Med Rep 14:3389-96.
24. Xu W, Lacerda L, Debeb BG, Atkinson RL, Solley TN, Li L, Orton D, McMurray JS, Hang BI, Lee E, Klopp AH, Ueno NT, Reuben JM, Krishnamurthy S, Woodward WA. 2013. The antihelmintic drug pyrvinium pamoate targets aggressive breast cancer. PLoS One 8:e71508.
25. Keyaerts E, Li S, Vijgen L, Rysman E, Verbeeck J, Van Ranst M, Maes P. 2009. Antiviralactivity of chloroquine against human coronavirus OC43 infection in newborn mice. Antimicrob Agents Chemother 53:3416-21.
26. Jacomy H, Talbot PJ. 2003. Vacuolating encephalitis in mice infected by human

564 coronavirus OC43. Virology 315: 20-33.
565 27. St-Jean JR, Jacomy H, Desforges M, Vabret A, Freymuth F, Talbot PJ. 2004. Human
566 respiratory coronavirus OC43: genetic stability and neuroinvasion. J Virol 78:8824–34.
567 28. Morfopoulou S, Brown JR, Davies EG, Anderson G, Virasami A, Qasim W, Chong WK,
568 Hubank M, Plagnol V, Desforges M, Jacques TS, Talbot PJ, Breuer J. 2016. Human
569 Coronavirus OC43 Associated with Fatal Encephalitis. N Engl J Med 375:497-8.
570 29. Yeh EA, Collins A, Cohen ME, Duffner PK, Faden H. 2004. Detection of coronavirus in
571 the central nervous system of a child with acute disseminated encephalomyelitis.
572 Pediatrics 113:e73-6.
573 30. Cheng VC, Lau SK, Woo PC, Yuen KY. 2007. Severe acute respiratory syndrome
574 coronavirus as an agent of emerging and reemerging infection. Clin Microbiol Rev
575 20:660-94.
576 31. Chan JF, Lau SK, To KK, Cheng VC, Woo PC, Yuen KY. 2015. Middle East respiratory
577 syndrome coronavirus: another zoonotic betacoronavirus causing SARS-like disease.
578 Clin Microbiol Rev 28:465–522.
579 32. Zumla A, Hui DS, Perlman S. 2015. Middle East respiratory syndrome. Lancet
580 386:995–1007.
581 33. Falzarano D, de Wit E, Martellaro C, Callison J, Munster VJ, Feldmann H. 2013.
582 Inhibition of novel β coronavirus replication by a combination of interferon-α2b and
583 ribavirin. Sci Rep 3:1686.
584 34. Hart BJ, Dyall J, Postnikova E, Zhou H, Kindrachuk J, Johnson RF. 2014. Interferon-β
585 and mycophenolic acid are potent inhibitors of Middle East respiratory syndrome

coronavirus in cell-based assays. J Gen Virol 9:571-7.

35. Yamamoto N, Yang R, Yoshinaka Y, Amari S, Nakano T, Cinatl J, Rabenau H, Doerr HW, Hunsmann G, Otaka A, Tamamura H, Fujii N, Yamamoto N. 2004. HIV protease inhibitor nelfinavir inhibits replication of SARS-associated coronavirus. Biochem Biophys Res Commun 18:719-25.

36. Chan JF, Chan KH, Kao RY, To KK, Zheng BJ, Li CP, Li PT, Dai J, Mok FK, Chen H, Hayden FG, Yuen KY. 2013. Broad-spectrum antivirals for the emerging Middle East respiratory syndrome coronavirus. J Infect 67:606-16.

37. Shin JS, Jung E, Kim M, Baric RS, Go YY. 2018. Saracatinib Inhibits Middle East Respiratory Syndrome-Coronavirus Replication In Vitro. Viruses 10:pii:E283.

38. Rabaan AA, Alahmed SH, Bazzi AM, Alhani HM. 2017. A review of candidate therapies for Middle East respiratory syndrome from a molecular perspective. J Med Microbiol 66:1261-74.

39. Agostini ML, Andres EL, Sims AC, Graham RL, Sheahan TP, Lu X, Smith EC, Case JB, Feng JY, Jordan R, Ray AS, Cihlar T, Siegel D, Mackman RL, Clarke MO, Baric RS, Denison MR. 2018. Coronavirus Susceptibility to the Antiviral Remdesivir (GS-5734) Is Mediated by the Viral Polymerase and the Proofreading Exoribonuclease. MBio 9:pii:e00221-18.

40. Channappanavar R, Lu L, Xia S, Du L, Meyerholz DK, Jiang S. 2015. Protective Effect of Intranasal Regimens Containing Peptidic Middle East Respiratory Syndrome Coronavirus Fusion Inhibitor Against MERS-CoV Infection J Infect Dis 212:1894-903.

41. Niu P, Zhang S, Zhou P, Huang B, Deng Y, Qin K, Wang P, Wang W, Wang X, Zhou J,

608 Zhang L, Tan W. 2018. Ultra-potent Human Neutralizing Antibody Repertoires Against
609 MERS-CoV from A Recovered Patient. J Infect Dis doi:10.1093/infdis/jiy311.
610 42. Jiang L, Wang N, Zuo T, Shi X, Poon KM, Wu Y, Gao F, Li D, Wang R, Guo J, Fu L,
611 Yuen KY, Zheng BJ, Wang X, Zhang L. 2014. Potent neutralization of MERS-CoV by
612 human neutralizing monoclonal antibodies to the viral spike glycoprotein. Sci Transl
613 Med. 6(234):234.
614 43. Lamoral-Theys D, Decaestecker C, Mathieu V, Dubois J, Kornienko A, Kiss R, Evidente
615 A, Pottier L. 2010. Lycorine and its derivatives for anticancer drug design. Mini Rev
616 Med Chem. 10:41-50.
617 44. Cedrón JC, Gutiérrez D, Flores N, Ravelo AG, Estévez-Braun A. 2010. Synthesis and
618 antiplasmodial activity of lycorine derivatives. Bioorg Med Chem 18:4694–701.
619 45. Toriizuka Y, Kinoshita E, Kogure N, Kitajima M, Ishiyama A, Otoguro K, Yamada H,
620 Omura S, Takayama H. 2008. New lycorine-type alkaloid from Lycoris traubii and
621 evaluation of antitrypanosomal and antimalarial activities of lycorine derivatives. Bioorg
622 Med Chem. 16:10182–9.
623 46. Hwang YC, Chu JJ, Yang PL, Chen W, Yates MV. 2008. Rapid identification of
624 inhibitors that interfere with poliovirus replication using a cell-based assay. Antiviral Res
625 77:232–6.
626 47. Li B, Wang Q, Pan X, Fernández de Castro I, Sun Y, Guo Y, Tao X, Risco C, Sui SF,
627 Lou Z. 2013. Bunyamwera virus possesses a distinct nucleocapsid protein to facilitate
628 genome encapsidation. Proc Natl Acad Sci U S A 110:9048–53.
629 48. Gabrielsen B, Monath TP, Huggins JW, Kefauver DF, Pettit GR, Groszek G. 1992.

Antiviral (RNA) activity of selected Amaryllidaceae isoquinoline constituents and synthesis of related substances. J Nat Prod 55:1569 –81.

49. Li SY, Chen C, Zhang HQ, Guo HY, Wang H, Wang L, Zhang X, Hua SN, Yu J, Xiao PG, Li RS, Tan X. 2005. Identification of natural compounds with antiviral activities against SARS-associated coronavirus. Antiviral Res 67:18–23.
50. Liu J, Yang Y, Xu Y, Ma C, Qin C, Zhang L. 2011. Lycorine reduces mortality of human enterovirus 71-infected mice by inhibiting virus replication. Virol J 8:483.
51. Guo Y, Wang Y, Cao L, Wang P, Qing J, Zheng Q, Shang L, Yin Z, Sun Y. 2015. A Conserved Inhibitory Mechanism of a Lycorine Derivative against Enterovirus and Hepatitis C Virus. Antimicrob Agents Chemother. 60:913–24.
52. He J, Qi WB, Wang L, Tian J, Jiao PR, Liu GQ, Ye WC, Liao M. 2013. Amaryllidaceae alkaloids inhibit nuclear-to-cytoplasmic export of ribonucleoprotein (RNP) complex of highly pathogenic avian influenza virus H5N1. Influenza and other respiratory viruses. 7:922-31.
53. Matthews H, Usman-Idris M, Khan F, Read M, Nirmalan N. 2013. Drug repositioning as a route to anti-malarial drug discovery: preliminary investigation of the in vitro anti-malarial efficacy of emetine dihydrochloride hydrate. Malar J. 12:359.
54. Low JSY, Chen KC, Wu KX, Ng ML, Chu JJH. 2009. Antiviral activity of emetine dihydrochloride against dengue virus infection. Journal of Antivirals & Antiretrovirals 1:62-71.
55. Chaves Valadão AL, Abreu CM, Dias JZ, Arantes P, Verli H, Tanuri A, de Aguiar RS.2015. Natural Plant Alkaloid (Emetine) Inhibits HIV-1 Replication by Interfering

652 with Reverse Transcriptase Activity. Molecules. 22;20(6):11474-89.
653 56. Khandelwal N, Chander Y, Rawat KD, Riyesh T, Nishanth C, Sharma S, Jindal N,
654 Tripathi BN, Barua S, Kumar N. 2017. Emetine inhibits replication of RNA and DNA
655 viruses without generating drug-resistant virus variants. Antiviral Res. 144:196-204.
656 57. MacGibeny MA, Koyuncu OO, Wirblich C, Schnell MJ, Enquist LW. 2018. Retrograde
657 axonal transport of rabies virus is unaffected by interferon treatment but blocked by
658 emetine locally in axons. PLoS Pathog. 14(7):e1007188.
659 58. Mukhopadhyay R, Roy S, Venkatadri R, Su YP, Ye W, Barnaeva E, Mathews Griner L,
660 Southall N, Hu X, Wang AQ, Xu X, Dulcey AE, Marugan JJ, Ferrer M, Arav-Boger R.
661 2016. Efficacy and Mechanism of Action of Low Dose Emetine against Human
662 Cytomegalovirus. PLoS Pathog. 12(6):e1005717.
663 59. Yang, Xu M, Lee EM, Gorshkov K, Shiryaev SA, He S, Sun W, Cheng YS, Hu X,
664 Tharappel AM, Lu B, Pinto A, Farhy C, Huang CT, Zhang Z, Zhu W, Wu Y, Zhou Y,
665 Song G, Zhu H, Shamim K, Martínez-Romero C, García-Sastre A, Preston RA,
666 Jayaweera DT, Huang R, Huang W, Xia M, Simeonov A, Ming G, Qiu X, Terskikh AV,
667 Tang H, Song H, Zheng W. 2018. Emetine inhibits Zika and Ebola virus infections
668 through two molecular mechanisms: inhibiting viral replication and decreasing viral
669 entry. Cell Discov. 4:31.
670 60. Chan JF, Yao Y, Yeung ML, Deng W, Bao L, Jia L, Li F, Xiao C, Gao H, Yu P, Cai JP,
671 Chu H, Zhou J, Chen H, Qin C, Yuen KY. 2015. Treatment With Lopinavir/Ritonavir or
672 Interferon-β1b Improves Outcome of MERS-CoV Infection in a Nonhuman Primate
673 Model of Common Marmoset. J Infect Dis 212:1904-13.

674 61. Alonso-Caplen FV, Matsuoka Y, Wilcox GE, Compans RW. 1984. Replication and
675 morphogenesis of avian coronavirus in Vero cells and their inhibition by monensin.
676 Virus Res 1:153-67.
677 62. Niemann H, Boschek B, Evans D, Rosing M, Tamura T, Klenk HD. 1982.
678 Post-translational glycosylation of coronavirus glycoprotein E1: inhibition by monensin.
679 EMBO J 1:1499-504.
680 63. Kim JC, Spence RA, Currier PF, Lu X, Denison MR. 1995. Coronavirus protein
681 processing and RNA synthesis is inhibited by the cysteine proteinase inhibitor e64dd.
682 Virology 208:1-8.
683 64. Lu R, Yu X, Wang W, Duan X, Zhang L, Zhou W, Xu J, Xu L, Hu Q, Lu J, Ruan L,
684 Wang Z, Tan W. Characterization of human coronavirus etiology in Chinese adults with
685 acute upper respiratory tract infection by real-time RT-PCR assays. PLoS One.
686 2012;7(6):e38638.
687 65. Corman VM, Müller MA, Costabel U, Timm J, Binger T, Meyer B, Kreher P, Lattwein
688 E, Eschbach-Bludau M, Nitsche A, Bleicker T, Landt O, Schweiger B, Drexler JF,
689 Osterhaus AD, Haagmans BL, Dittmer U, Bonin F, Wolff T, Drosten C. 2012. Assays for
690 laboratory confirmation of novel human coronavirus (hCoV-EMC) infections. Euro
691 Surveill 17:pii: 20334.
692 66. Lan J, Yao Y, Deng Y, Chen H, Lu G, Wang W, Bao L, Deng W, Wei Q, Gao GF, Qin
693 C, Tan W. 2015. Recombinant receptor binding domain protein induces partial protective
694 immunity in rhesus macaques against Middle East respiratory syndrome coronavirus
695 challenge. EBioMedicine 2:1438–46.
696

Figure 1. Screening for anti-HCoV-OC43 compounds. (A) Schematic of the HTS assay. BHK-21 cells were seeded in 96-well plates, and after a 24-h incubation (~10,000 cells/well), the medium was replaced with 94 μL DMEM supplemented with 3% FBS. The cells were treated in triplicate with 1 μL of each compound (diluted in DMSO) at a final concentration of 10 μM. After 1 h, 5 μL of rOC43ns2DelRluc was added, and the cells were cultured for an additional 72 h, after which Rluc activity, represented as relative light units (RLUs), was measured. Screened compounds were confirmed using HCoV-OC43-WT. (B) Overview of HTS and the confirmation assay. All compounds and their corresponding activity are displayed as squares. The percentage inhibition of Rluc activity of rOC43ns2DelRluc is displayed along the vertical axis versus the percentage inhibition of BHK-21 proliferation displayed along the horizontal axis. Compounds exhibiting >70% inhibition of Rluc activity and <80% cytotoxicity were considered effective inhibitors of rOC43ns2DelRluc and are displayed in red and yellow (yellow squares represent the compounds screened in the HTS using rOC43ns2DelRluc and confirmed using HCoV-OC43-WT), with the ineffective compounds displayed in gray. Data represent the mean ± standard deviation of three replicates. The screening assay was repeated at least three times.

Figure 2. Dose–response curves for seven broad-spectrum inhibitors of four types of CoVs *in vitro*. BHK-21, Vero E6, LLC-MK2, or DBT cells were infected with HCoV-OC43-WT, MERS-CoV, HCoV-NL63, or MHV-A59 at an MOI of 0.01, respectively, and treated for 72 h with eight doses (0.1, 0.25, 0.5, 1, 2, 5, 10, or 20 μM) of lycorine (A), emetine (B), mycophenolate mofetil (C), phenazopyridine (D), mycophenolic acid (E),

719 pyrvinium pamoate (F), or monensin sodium (G). At 72-h post-infection, the cell-culture
720 supernatants were subjected to a viral-load assay, and cell lysates were assessed for
721 cytotoxicity. Percent inhibition was calculated as inhibition of viral load (%) = 100% − [viral
722 load (titers or copies) of each CoV in the compound-treated cells / viral load of
723 DMSO-treated control cells]. Inhibition is shown in red, and cytotoxicity is shown in blue.
724 EC_{50} values and SI (CC_{50}/EC_{50}) are shown. Data represent the mean ± standard deviation
725 (error bars) of three independent experiments.

726

727 **Figure 3. Confirmation of anti-CoV activity by IFA and western blot.** (A) IFA of the
728 HCoV-OC43 nucleocapsid (N) protein in inhibitor-treated BHK-21 cells. BHK-21 cells in
729 96-well plates were infected with HCoV-OC43-WT (MOI = 0.01) in the presence of 10 μM
730 of the indicated inhibitors, with chloroquine and DMSO used as the positive and negative
731 controls, respectively. At 72-h post-infection, the cells were analyzed by IFA for N protein
732 (green) expression. Nuclei (blue) were stained with DAPI. (B) Effect of the inhibitors on N
733 protein synthesis by HCoV-OC43-WT was determined by western blot. BHK-21 cells in
734 12-well plates were infected with HCoV-OC43-WT (MOI = 0.01) in the presence of 10 μM
735 of the indicated inhibitors, with chloroquine and DMSO used as the positive and negative
736 controls, respectively. At 72-h post-infection, cells were analyzed by western blot using
737 antibodies against HCoV-OC43 N protein and β-actin.

738

739 **Figure 4. Emetine strongly inhibited MERS-CoV entry.** DPP4-expressing Huh7.5 cells

740 were cultured with 200 $TCID_{50}$ pseudotyped MERS-CoV in the presence of serial
741 concentrations of individual inhibitors. Inhibition percentage was calculated by measuring the
742 luciferase expression of the inhibitor-treated cells relative to that in DMSO-treated cells. Data
743 represent the mean ± standard deviation of three replicates.

744

745 **Figure 5. Lycorine protects mice against HCoV-OC43 infection**. (A) Kaplan–Meier
746 survival curves of mice >20 days after intranasal inoculation of HCoV-OC43, followed by
747 treatment with the indicated inhibitors (*n* = 6/group). Inhibitor doses and regimens were
748 selected based on their acute toxicity (emetine was used at 5 mg/kg, chloroquine was used at
749 30 mg/kg, and the other inhibitors were used at 15 mg/kg). (B) Viral loads in the mouse brain
750 and spinal cord treated with lycorine. Twelve-day-old female BALB/c mice were inoculated
751 via the intranasal route with 100 $TCID_{50}$ HCoV-OC43-WT and treated with lycorine or
752 DMSO control for 3 days. At 72-h post-infection, viral loads in the mouse brain and spinal
753 cord were determined by qRT-PCR. Data represent the mean ± standard deviation (error bars)
754 of three independent experiments. (C) IHC analyses of brain tissue from mice treated with
755 lycorine. Twelve-day-old female BALB/c mice were inoculated via the intranasal route with
756 100 $TCID_{50}$ HCoV-OC43-WT and treated with lycorine or DMSO control for 3 days. Mouse
757 brain coronal sections were stained for HCoV-OC43 N (green) and nuclei (blue).

758

759 **Figure 6. Lycorine inhibited the spread of rOC43-ns2Del-Rluc in the mouse brain**. (A)
760 Representative dorsal images of 12-day-old female BALB/c mice administered 15 mg/kg

lycorine in DMSO/PBS or DMSO/PBS alone daily after inoculation with rOC43-ns2Del-Rluc. At 2-, 3-, and 4-days post-inoculation, mice were processed for BLI, with the results displayed as a heat map. (B) Rluc activity of rOC43-ns2Del-Rluc in the mouse brain at 72-h post-inoculation. Data represent the mean ± standard deviation (error bars) of three independent experiments. $^{**}p < 0.01$.

Figure 1

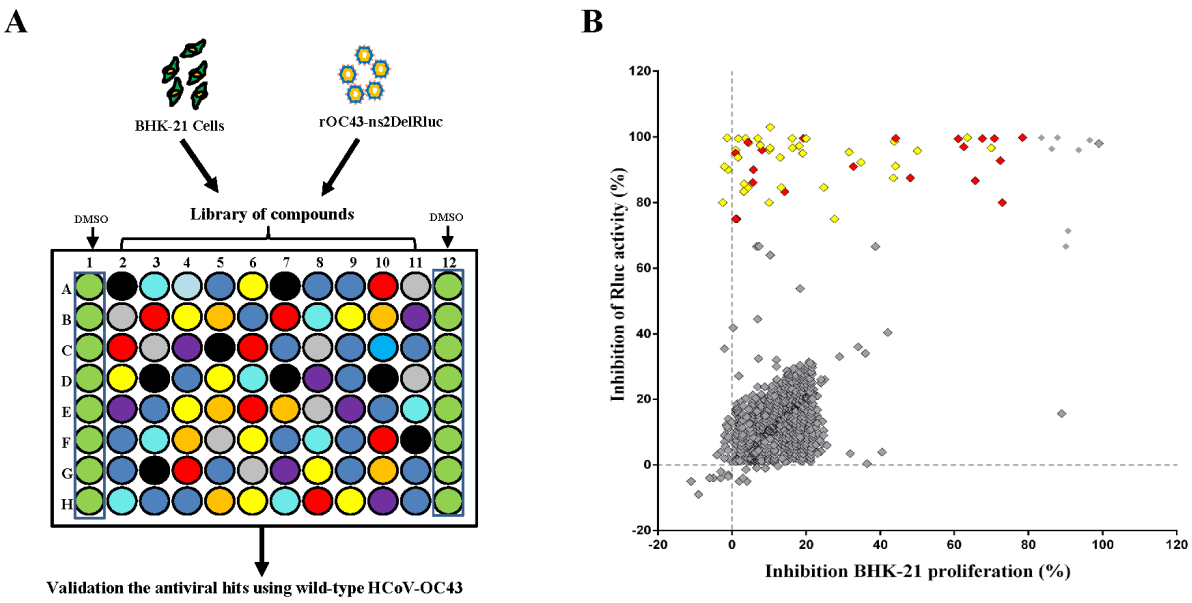

Figure 2

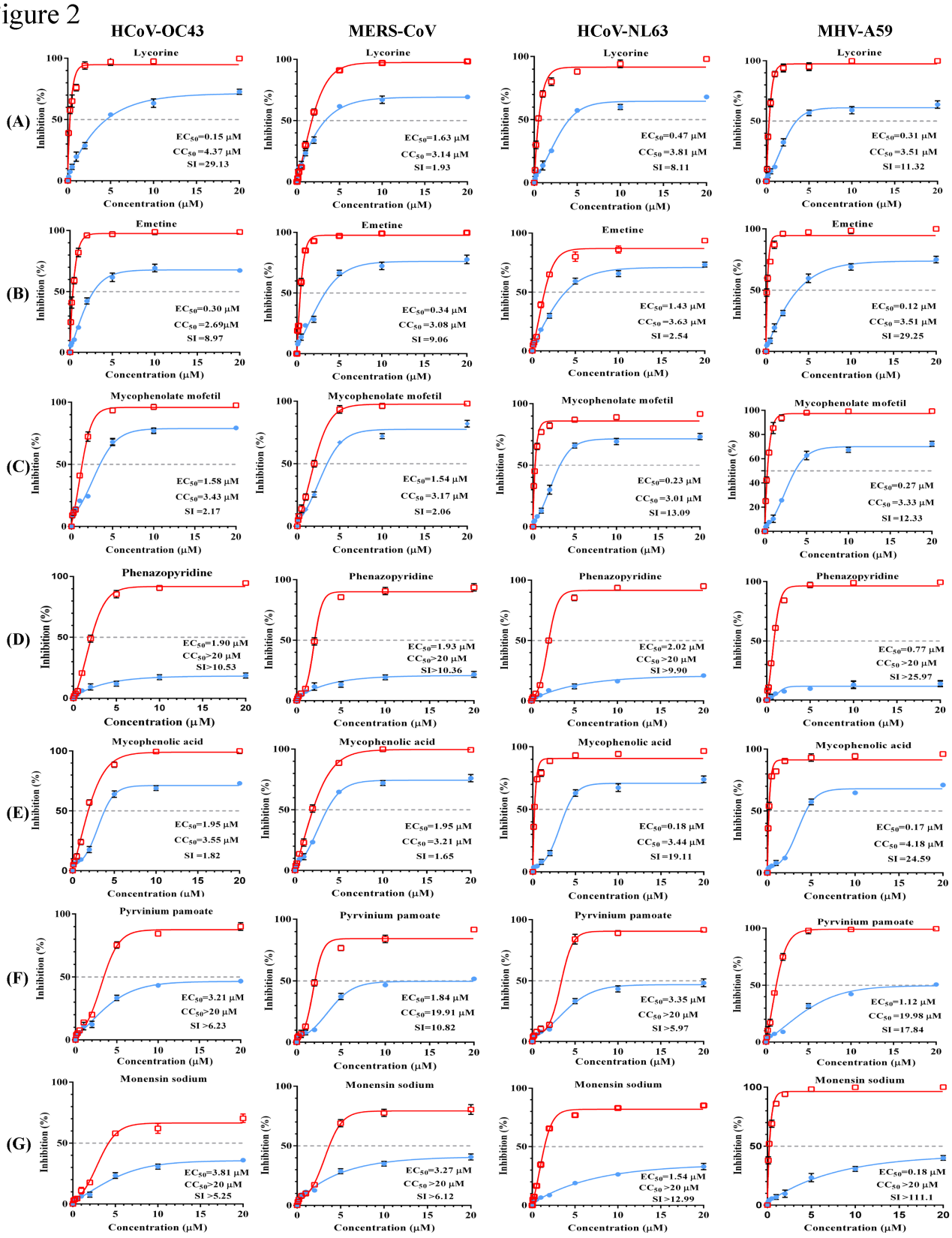

Figure 3

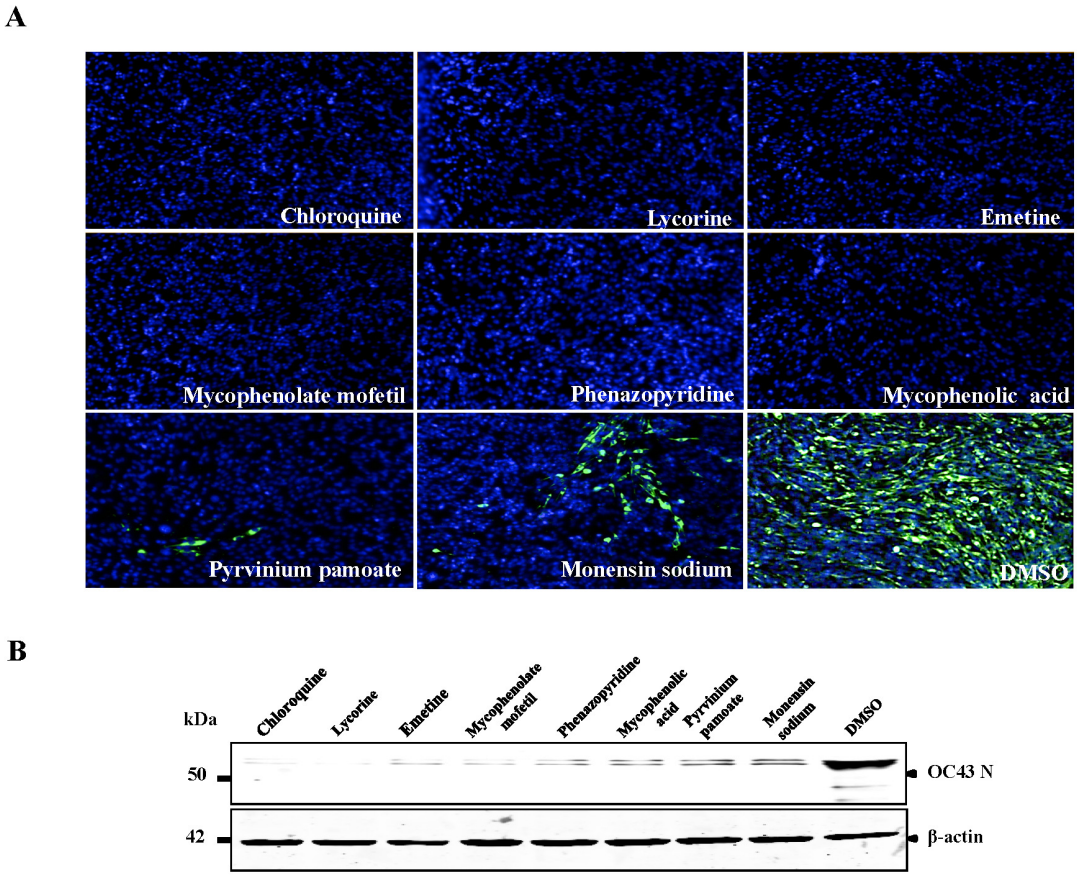

Figure 4

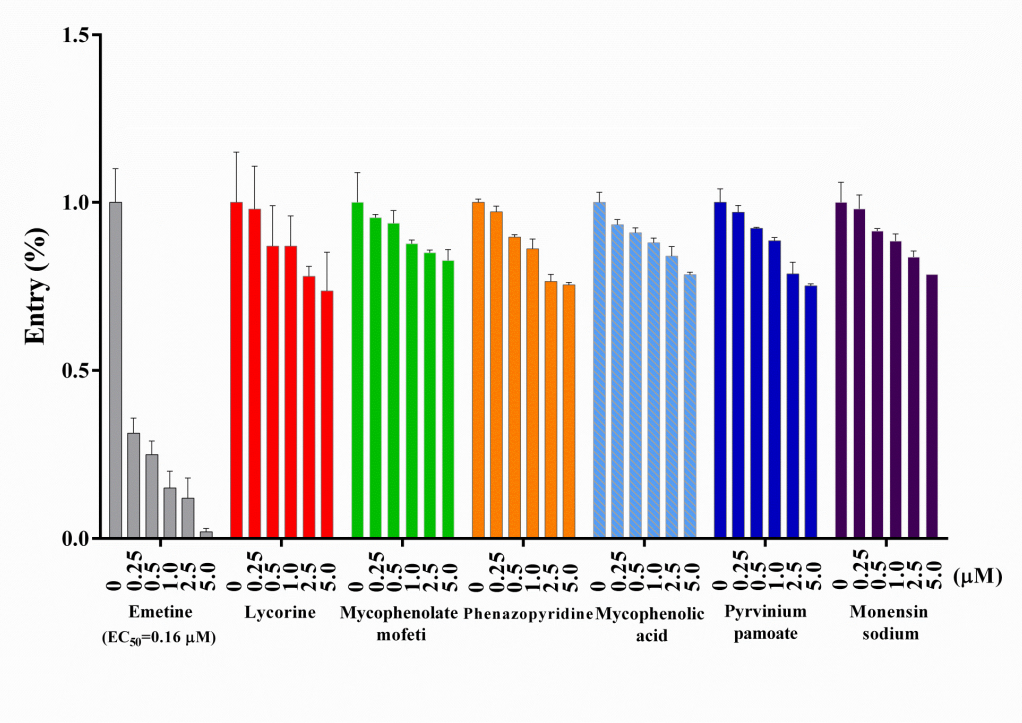

Figure 5

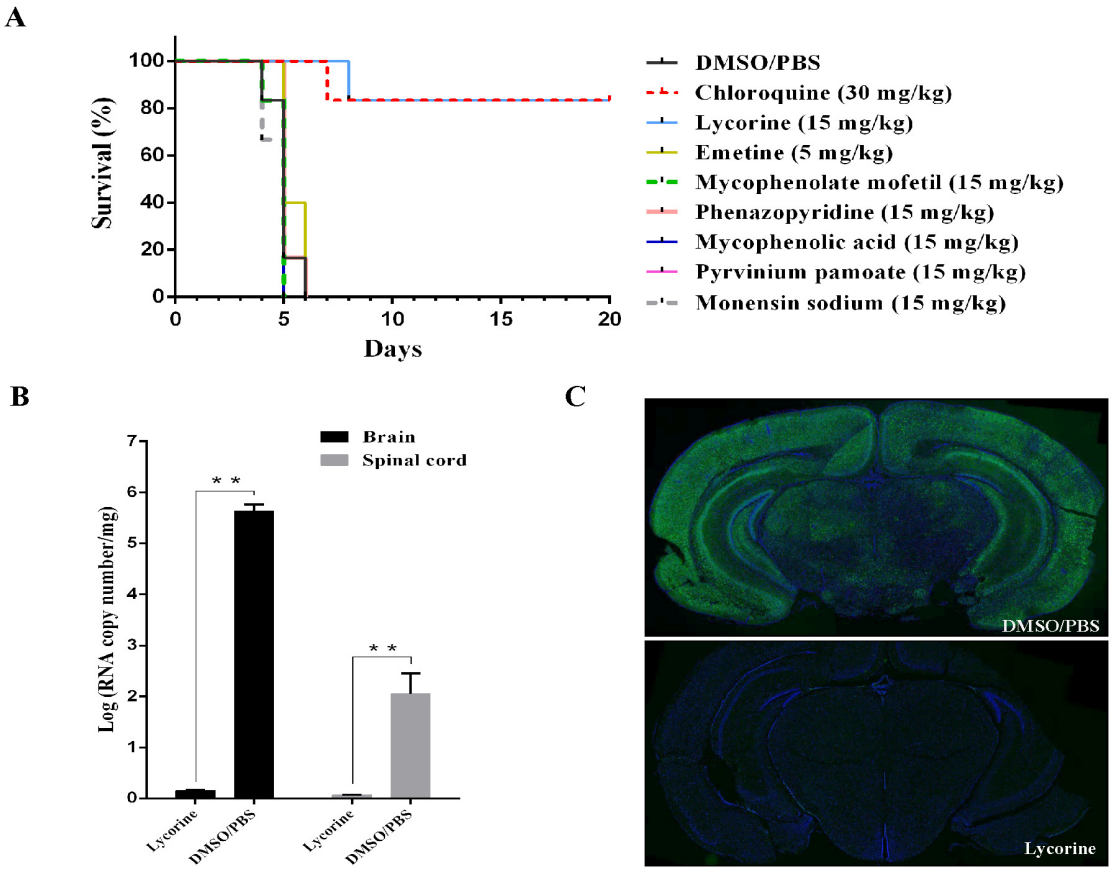

Figure 6

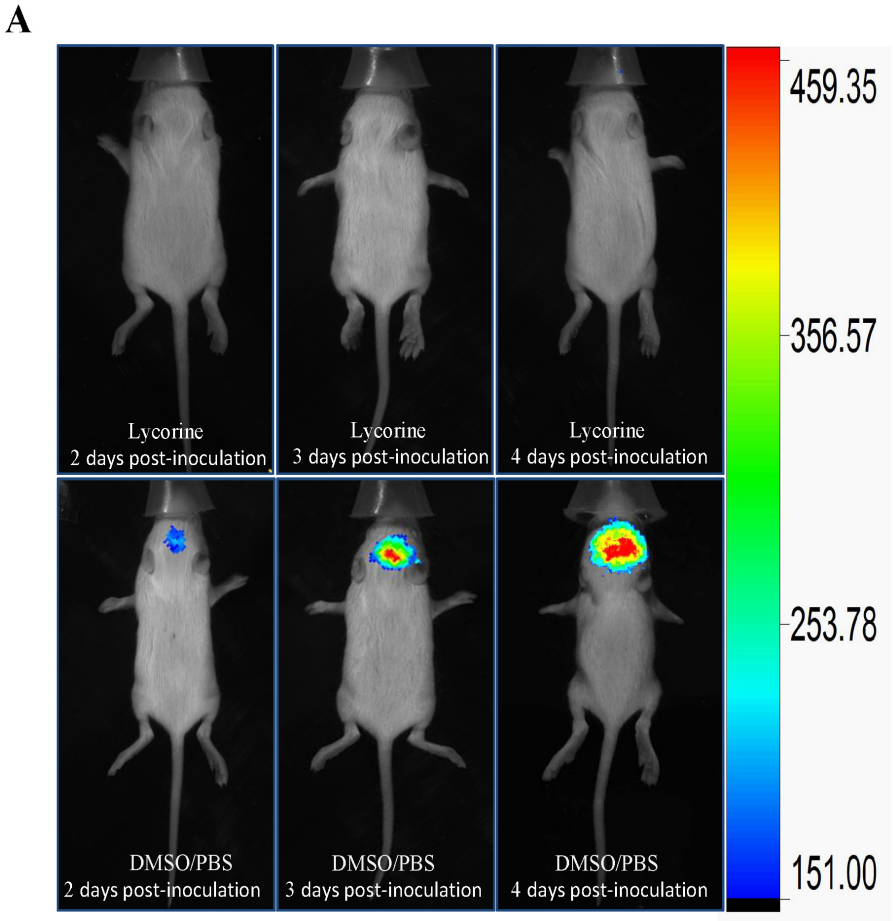

Table 1. Properties and antiviral activities of 36 compounds against four CoVs.

Compound name	CAS number	Formula	Bioactivity	HCoV-OC43 EC_{50} and CC_{50}	HCoV-NL63 EC_{50} and CC_{50}	MERS-CoV EC_{50} and CC_{50}	MHV-A59 EC_{50} and CC_{50}
Lycorine	476-28-8	$C_{16}H_{17}NO_4$	Inhibits cell division, antineoplastic, antiviral	EC_{50}=0.15 CC_{50}=4.37	EC_{50}=0.47 CC_{50}=3.81	EC_{50}=1.63 CC_{50}=3.14	EC_{50}=0.31 CC_{50}=3.51
Emetine	483-18-1	$C_{29}H_{42}C_{l2}N_2O_4$	Inhibits RNA, DNA and protein synthesis	EC_{50}=0.30 CC_{50}=2.69	EC_{50}=1.43 CC_{50}=3.63	EC_{50}=0.34 CC_{50}=3.08	EC_{50}=0.12 CC_{50}=3.51
Mycophenolatemofeti	115007-34-6	$C_{23}H_{31}NO_7$	Immune suppressant, antineoplastic, antiviral	EC_{50}=1.58 CC_{50}=3.43	EC_{50}=0.23 CC_{50}=3.01	EC_{50}=1.54 CC_{50}=3.17	EC_{50}=0.27 CC_{50}=3.33
Phenazopyridine	94-78-0	$C_{11}H_{12}ClN_5$	Analgesic	EC_{50}=1.90 CC_{50}>20	EC_{50}=2.02 CC_{50}>20	EC_{50}=1.93 CC_{50}>20	EC_{50}=0.77 CC_{50}>20
Mycophenolic acid	24280-93-1	$C_{17}H_{20}O_6$	Immune suppressant, antineoplastic, antiviral	EC_{50}=1.95 CC_{50}=3.55	EC_{50}=0.18 CC_{50}=3.44	EC_{50}=1.95 CC_{50}=3.21	EC_{50}=0.17 CC_{50}=4.18
Pyrviniumpamoate	3546-41-6	$C_{49}H_{43}N_3O_6$	Anthelmintic	EC_{50}=3.21 CC_{50}>20	EC_{50}=3.35 CC_{50}>20	EC_{50}=1.84 CC_{50}=19.91	EC_{50}=4.12 CC_{50}=19.98
Monensin sodium	22373-78-0	$C_{37}H_{63}NaO_{10}$	Antibacterial	EC_{50}=3.81 CC_{50}>20	EC_{50}=1.54 CC_{50}>20	EC_{50}=3.27 CC_{50}>20	EC_{50}=0.18 CC_{50}>20
Cycloheximide	66-81-9	$C_{15}H_{23}NO_4$	Protein synthesis inhibitor	EC_{50}=0.43 CC_{50}=3.12	EC_{50}=2.64 CC_{50}=3.24	EC_{50}=2.56 CC_{50}=2.96	EC_{50}=5.21 CC_{50}=3.19
Cetylpyridinium chloride	6004-24-6	$C_{21}H_{38}ClN$	Antiinfective	EC_{50}=4.31 CC_{50}=8.23	EC_{50}=1.24 CC_{50}=8.52	EC_{50}=0.69 CC_{50}=8.14	EC_{50}=7.86 CC_{50}=8.19
Oligomycin	1404-19-9	$C_{45}H_{74}O_{11}$	Antibacterial, antifungal	EC_{50}=0.19 CC_{50}=6.56	EC_{50}=2.63 CC_{50}=4.26	EC_{50}=0.21 CC_{50}=5.16	EC_{50}=6.43 CC_{50}=6.78
Promazine	58-40-2	$C_{17}H_{21}ClN_2S$	Antipsychotic	EC_{50}=0.41 CC_{50}>20	EC_{50}=1.37 CC_{50}>20	EC_{50}=13.72 CC_{50}>20	EC_{50}=0.51 CC_{50}>20
Diperodon	537-12-2	$C_{22}H_{28}ClN_3O_4$	Analgesic, anesthetic	EC_{50}=1.71 CC_{50}=14.3	EC_{50}=4.91 CC_{50}=13.6	EC_{50}=8.77 CC_{50}=14.2	EC_{50}=1.98 CC_{50}=14.5
Dihydrocelastryl diacetate	NOcas#	$C_{33}H_{44}O_6$	Antibacterial	EC_{50}=1.71 CC_{50}>20	EC_{50}=0.65 CC_{50}>20	EC_{50}=10.58 CC_{50}>20	EC_{50}=4.24 CC_{50}>20
Tetrandrine	518-34-3	$C_{38}H_{42}N_2O_6$	Analgesic, antineoplastic, antihypertensive	EC_{50}=0.29 CC_{50}>20	EC_{50}=2.05 CC_{50}>20	EC_{50}=12.68 CC_{50}>20	EC_{50}=4.81 CC_{50}>20
Pristimerin	1258-84-0	$C_{30}H_{40}O_4$	Antineoplastic, antiinflammatory	EC_{50}=1.99 CC_{50}>20	EC_{50}=1.63 CC_{50}>20	EC_{50}=13.87 CC_{50}>20	EC_{50}=9.17 CC_{50}>20
Chloroquine	54-05-7	$C_{18}H_{32}ClN_3O_8P_2$	Antimalarial, antiamebic, antirheumatic	EC_{50}=0.33 CC_{50}>20	EC_{50}=4.89 CC_{50}>20	EC_{50}=16.44 CC_{50}>20	EC_{50}=15.92 CC_{50}>20
Valinomycin	2001-95-8	$C_{54}H_{90}N_6O_{18}$	Antibiotic	EC_{50}=4.43 CC_{50}=6.15	EC_{50}=1.89 CC_{50}=4.12	EC_{50}=6.07 CC_{50}=5.88	EC_{50}=6.78 CC_{50}=5.11
Loperamide	34552-83-5	$C_{29}H_{34}Cl_2N_2O_2$	Ca channel blocker	EC_{50}=1.86 CC_{50}=18.7	EC_{50}=6.47 CC_{50}=18.27	EC_{50}=4.82 CC_{50}=18.9	EC_{50}=10.65 CC_{50}=18.9
Harmine	442-51-3	$C_{13}H_{12}N_2O$	Antiparkinsonian, CNS stimulant	EC_{50}=1.90 CC_{50}>20	EC_{50}=13.46 CC_{50}>20	EC_{50}=4.93 CC_{50}>20	EC_{50}=13.77 CC_{50}>20

Conessine	546-06-5	$C_{24}H_{40}N_2$	Antimalarial, antihistamine	EC_{50}=2.34 CC_{50}>20	EC_{50}=10.75 CC_{50}>20	EC_{50}=4.98 CC_{50}>20	EC_{50}=11.46 CC_{50}>20
Chloropyramine	6170-42-9	$C_{16}H_{21}Cl_2N_3$	Antihistamine	EC_{50}=1.79 CC_{50}>20	EC_{50}=14.21 CC_{50}>20	EC_{50}=14.21 CC_{50}>20	EC_{50}=2.42 CC_{50}>20
Doxazosin mesylate	77883-43-3	$C_{24}H_{29}N_5O_8S$	Antihypertensive	EC_{50}=4.97 CC_{50}>20	EC_{50}=13.95 CC_{50}>20	EC_{50}=12.66 CC_{50}>20	EC_{50}=14.48 CC_{50}>20
Alprenolol	13655-52-2	$C_{15}H_{24}ClNO_2$	Beta-adrenergic blocker	EC_{50}=1.95 CC_{50}>20	EC_{50}=11.88 CC_{50}>20	EC_{50}=10.53 CC_{50}>20	EC_{50}=13.97 CC_{50}>20
Berbamine	478-61-5	$C_{37}H_{42}Cl_2N_2O_6$	Antihypertensive, skeletal muscle relaxant	EC_{50}=1.48 CC_{50}>20	EC_{50}=9.46 CC_{50}>20	EC_{50}=13.14 CC_{50}>20	EC_{50}=10.91 CC_{50}>20
Phenylmercuric acetate	62-38-4	$C_8H_8HgO_2$	Antifungal	EC_{50}=2.17 CC_{50}=5.35	EC_{50}=6.79 CC_{50}=5.47	EC_{50}=6.44 CC_{50}=5.39	EC_{50}=6.81 CC_{50}=5.97
Hycanthone	3105-97-3	$C_{20}H_{24}N_2O_2S$	Anthelmintic, hepatotoxic	EC_{50}=0.16 CC_{50}=3.58	EC_{50}=5.76 CC_{50}=3.68	EC_{50}=5.11 CC_{50}=4.32	EC_{50}=5.78 CC_{50}=4.19
Zoxazolamine	61-80-3	$C_7H_5ClN_2O$	Muscle relaxant, antirrheumatic	EC_{50}=1.39 CC_{50}>20	EC_{50}=13.51 CC_{50}>20	EC_{50}=14.21 CC_{50}>20	EC_{50}=16.45 CC_{50}>20
Ticlopidine	53885-35-1	$C_{14}H_{15}Cl_2NS$	PAF inhibitor	EC_{50}=1.41 CC_{50}>20	EC_{50}=15.65 CC_{50}>20	EC_{50}=11.25 CC_{50}>20	EC_{50}=14.28 CC_{50}>20
4'-hydroxychalcone	2657-25-2	$C_{15}H_{12}O_2$	Antineoplastic	EC_{50}=1.52 CC_{50}>20	EC_{50}=7.25 CC_{50}>20	EC_{50}=10.23 CC_{50}>20	EC_{50}=9.75 CC_{50}>20
Papaverine	61-25-6	$C_{20}H_{22}ClNO_4$	Muscle relaxant, cerebral vasodilator	EC_{50}=1.61 CC_{50}=12.11	EC_{50}=7.32 CC_{50}=11.71	EC_{50}=9.45 CC_{50}=11.98	EC_{50}=11.46 CC_{50}=12.44
Propranolol	318-98-9	$C_{16}H_{22}ClNO_2$	Antihypertensive,antian ginal,antiarrhythmic	EC_{50}=0.48 CC_{50}>20	EC_{50}=8.11 CC_{50}>20	EC_{50}=11.01 CC_{50}>20	EC_{50}=13.54 CC_{50}>20
Tilorone	27591-69-1	$C_{25}H_{34}N_2O_3$	Antiviral	EC_{50}=0.32 CC_{50}>20	EC_{50}=6.89 CC_{50}>20	EC_{50}=10.56 CC_{50}>20	EC_{50}=16.11 CC_{50}>20
Antimycin A	1397-94-0	$C_{27}H_{38}N_2O_9$	Antifungal, antiviral, interferes in cytochrome oxidation	EC_{50}=1.65 CC_{50}=3.62	EC_{50}=6.05 CC_{50}=4.21	EC_{50}=6.89 CC_{50}=4.32	EC_{50}=5.42 CC_{50}=3.98
Salinomycin sodium	53003-10-4	$C_{42}H_{69}NaO_{11}$	Antibacterial	EC_{50}=0.29 CC_{50}=1.97	EC_{50}=5.71 CC_{50}=2.41	EC_{50}=5.49 CC_{50}=3.84	EC_{50}=5.16 CC_{50}=2.45
Exalamide	53370-90-4	$C_{13}H_{19}NO_2$	Antifungal	EC_{50}=1.48 CC_{50}>20	EC_{50}=17.49 CC_{50}>20	EC_{50}=15.91 CC_{50}>20	EC_{50}=16.39 CC_{50}>20
Desipramine	50-47-5	$C_{18}H_{23}ClN_2$	Antidepressant	EC_{50}=1.67 CC_{50}>20	EC_{50}=6.68 CC_{50}>20	EC_{50}=11.59 CC_{50}>20	EC_{50}=8.75 CC_{50}>20